INSTITUTE OF THEORETICAL
AND EXPERIMENTAL PHYSICS

V.S.Popov, V.D.Mur, A.V.Sergeev,
V.M.Weinberg

THE STARK EFFECT IN INTENSE FIELD. II

Preprint №177

Moscow — ATOMINFORM — 1987

УДК 539.I М-I6

THE STARK EFFECT IN INTENSE FIELD. II; Preprint ITEP 87-177/
V.S.Popov, V.D.Mur, A.V.Sergeev, V.M.Weinberg - M.: ATOMINFORM, 1987 - 37p.

The problem of hydrogen atom in homogeneous electric field is considered. The Stark shifts and widths of atomic levels are computed by summation of divergent perturbation series and by 1/n-expansion - up to $\mathcal{E}$ values comparable with the field on the electron orbit. The results of the calculations are presented for the following sequences of states : $|n_1,0,0\rangle$, $|0,n_2,0\rangle$, $|n_1,n_1,0\rangle$, as well as for all states with n = 2 and 3 (n is the principal quantum number). The Stark shifts and widths of Rydberg states (with n = 15÷30) in electric field which exceeds the classical ionization threshold are computed. The results of our calculations agree with experiment.

Fig. - 12, ref.- 32

1. The Stark effect in hydrogen atom was studied by many authors, see e.g. [1-20] and further references in [1,4,14] but they considered only the region of a relatively small field. Nowadays, owing to a progress in atomic physics and laser spectroscopy, it seems to be essential to calculate Stark shifts and widths for a wide variety of states, including Rydberg states ($n >> 1$).

The homogeneous electric field $\mathcal{E}$ takes off the "accidental" degeneracy of hydrogen atom states (at $\mathcal{E} \neq 0$ the level with parabolic quantum numbers n_1, n_2, m splits into $n(n+1)/2$ sublevels). At switching in the field, the discrete spectrum state $|n_1, n_2, m\rangle$ goes over into a quasistationary state with the complex energy $E = E_0 - i\Gamma/2$ which will be denoted by the same quantum numbers. Instead of energy E and field $\mathcal{E}$ we shall use the "reduced" variables [1]:

$$\varepsilon^{(n_1 n_2 m)}(\mathcal{E}) = \varepsilon' - i\varepsilon'' = 2n^2(E_0 - i\Gamma/2), \quad F = n^4\mathcal{E} \qquad (1)$$

which is especially convenient for the case of Rydberg states (for simplicity we call ε'_n and $\varepsilon''_n = n^2\Gamma^{(n_1 n_2 m)}$ the shift and width too). In this work, which is a direct continuation of ref. [20], we present the results of computation of $\varepsilon^{(n_1 n_2 m)}$ in strong fields (up to $F \sim 1$) for different states of a hydrogen atom.

2. Calculation methods. We used two independent calculation methods: 1) The summation of Rayleigh-Schrödinger perturbation series (PS)

$$\varepsilon^{(n_1 n_2 m)} = \sum_{k=0}^{\infty} \varepsilon_k^{(n_1 n_2 m)} F^k \qquad (2)$$

2) 1/n-expansion for the energy eigenvalues,

$$\varepsilon = \varepsilon^{(0)} + \frac{\varepsilon^{(1)}}{n} + \frac{\varepsilon^{(2)}}{n^2} + \dots \qquad (3)$$

Let us briefly describe these methods.

As follows from PS analysis, the coefficients ε_k in eq. (2) have the following structure:

$$\varepsilon_k = \begin{cases} P_k(x^2, \mu^2, 1/n^2) & , \text{ k - even} \\ x P_k(x^2, \mu^2, 1/n^2) & , \text{ k - odd} \end{cases} \qquad (4)$$

where k is the perturbation theory (PT) order, $x = (n_1 - n_2)/n$, $\mu = m/n$ and P_k is a polynomial of degree $[k/2]$. For instance [6-10],

$$P_0 = -1 , \quad P_1 = 3 , \quad P_2 = -\frac{1}{8}(17 - 3x^2 - 9\mu^2 + 19 n^{-2}) ,$$

$$P_3 = \frac{3}{16}(23 - x^2 + 11\mu^2 + 39 n^{-2}),$$

$$P_4 = -\frac{1}{512}[5487 + 1806x^2 - 3402\mu^2 - 1134 x^2\mu^2 + 147 x^4 - 549\mu^4 + (35182 + 5754x^2 - 8622\mu^2) n^{-2} + 16211 n^{-4}] , \dots$$

Recently, owing to development of new PT technique, a great number of PT coefficients ε_k has been computed [7-9], up to k = 160 for the ground state, up to k = 100 for the states with n =2 and so on. However, the series (2) have zero convergence radius because higher order PT series factorially grow at $k \to \infty$ (the Dyson phenomenon [21]):

$$\varepsilon_k^{(n_1 n_2 m)} \approx k!\, a^k k^\beta \left(b_0 + \frac{b_1}{k} + \frac{b_2}{k^2} + \ldots\right) \qquad (5)$$

In the case of the Stark effect $a = 3/2n$, $\beta = n + |n_1 - n_2| - 1$ and, e.g., for states with $n_1 = n_2$

$$b_0 = -\frac{6^n}{\pi n^3 \left(\frac{n+m-1}{2}\right)! \left(\frac{n-m-1}{2}\right)!} \cdot \frac{1+(-1)^k}{2}, \quad m = n-1, n-3, \ldots, 0 \text{ or } 1.$$

To compute the energy eigenvalue from PS coefficients one may use the conventional PT polynomials

$$S_N(\mathcal{E}) = \sum_{k=0}^{N} E_k^{(n_1 n_2 m)} \mathcal{E}^k \qquad (6)$$

However, since PS diverge at any $\mathcal{E} > 0$, such an attempt may be successful only at small $\mathcal{E}$ and even in this region, because the coefficients E_k are real, the polynomials (6) determine only the Stark shift, not the width of the level.

To advance into the strong field region, $F \gtrsim 1$, one must sum the divergent PS series. To this end we have used the Hermite-Padé approximants (HPA), the solutions of which $y_N(F)$ are calculated from the equation $P_N - Q_N y + R_N y^2 = 0$ (7)

Here $P_N(F)$, $Q_N(F)$ and $R_N(F)$ are polynomials of degree N the coefficients of which are unambiguously determined from PS coefficients through the condition

$$P_N - Q_N E + R_N E^2 = O(F^{3N+2}), \quad F \to 0, \qquad (7')$$

where $E = E(F)$ is PS (2). The ordinary Padé approximants $[N/N](F)$ are a particular case of (7') with $R_N \equiv 0$. It is clear that $y_N(F)$ contrary to $[N/N](F)$ may have imaginary part (at real F) even if all coefficients of polynomials P_N, Q_N and R_N are real which is just the case in the Stark effect problem. This fact determines a considerable advantage of HPA against PA in the case of PS summation for the Stark effect. Investigation of convergence of the sequence y_N with N increasing indicates that at $N \sim 10 \div 12$ the values of $y_N(F)$ are stabilized and the precision in energy evaluation not less than 10^{-4} is achieved.

3. The other approach is based on the 1/n-expansion which is nowadays successfully applied in quantum mechanics and field theory. This method was applied to Stark effect for states $|0,0,n-1\rangle$, which correspond in the classical $n \to \infty$ limit to the circular electron orbit, in refs.[17,20]. In doing so, the first term $\mathcal{E}^{(0)}$ of expansion (3) is completely determined by the stable equilibrium point for a classical particle in the effective potential including centrifugal energy and succeeding coefficients $\mathcal{E}^{(k)}$, $k \geq 1$, are calculated by recurrence relations. Unlike PS coefficients $\mathcal{E}_k$, the 1/n-expansion coefficients $\mathcal{E}^{(k)}$ depend themselves on the field F and in a rather complicated manner. Nevertheless, it is not difficult to calculate them numerically.

Referring for details to ref.[20], we present here only an equation for $\mathcal{E}^{(0)}$. The F-dependence for the Stark-effect problem is given as follows:

$$\mathcal{E}^{(0)} = -(1-\tau^2)^2(1+3\tau^2), \qquad \tau(1-\tau^2)^4 = F, \tag{8}$$

$\tau = \tau(F)$ is the root of equation which tends to zero at $F \to 0$. Note that variable τ has simple geometrical meaning: $\tau = z/r$, where z and r refer to the classical orbit (see Fig.1 in [20]).

It is easy to see from eq.(8) that at $\tau = 1/3$, or

$$F = F_* = 2^{12}\cdot 3^{-9} = 0.2081, \qquad \mathcal{E}^{(0)} = \mathcal{E}_* = -\frac{256}{243} \tag{9}$$

a "clash" of two classical solutions occurs, one of them corresponding to stable and the other to unstable equilibrium points. At $F > F_*$ the effective potential has no minima at real values of coordinates ξ and η. In other words, the equilibrium point escapes to the comples plane. Such a solution has no physical meaning in classical mechanics but in quantum mechanics it is just the solution which allows one to describe not only the shift but the width of the levels as well[20].

We apply[17,20] the 1/n-expansion to nodeless states ($n_1 = n_2 = 0$) which correspond in the classical ($n \to \infty$) limit to the circular electron orbits normal to the direction of the field $\mathcal{E}$ (this approach can be easily generalized to the case $n_1, n_2 \ll n$). Excluding the region of F close to F_*, the 1/n-expansion determines the energy $\mathcal{E} = \mathcal{E}' - i\,\mathcal{E}''$ with a good accura-

cy at $n \geqslant 5$ and after summing up series (3) by Padè-approximants $[N/N]\,(1/n)$, even for the ground state, n=1.

The HPA method has advantages at $F \lesssim 0.3$ and small n . It is essential that there is an overlapping region where both methods agree with each other and at $F \leq 0.1$ - with the other calculations[5,15,16].

For further details about computational methods, their convergence rates and so on we refer to ref.[20].

4. Turning to the results of the calculation we describe first the Stark shifts $\varepsilon_n' = 2n^2 \mathrm{Re}\, E^{(n_1 n_2 m)}$ and in the next Section - the Stark widths. We will not reproduce here the results for the states $|0,0,n-1\rangle$ since they have been published earlier[17, 20].

Consider two sets of states, $|n-1,0,0\rangle$ and $|0,n-1,0\rangle$ the first of which correspond to the widest and the second - to the narrowest among all sublevels with given n . Here the sign of the Stark shift is determined by the first PS term: it is positive for $|n-1,0,0\rangle$ states and negative for $|0,n-1,0\rangle$ states, see Fig.1. But as a whole, the F-dependence of ε_n' is far enough from linear.

Note that due to symmetry relations[10]

$$\varepsilon_k^{(n_2 n_1 m)} = (-1)^k \varepsilon_k^{(n_1 n_2 m)}, \qquad \varepsilon^{(n_2 n_1 m)}(-F) = \varepsilon^{(n_1 n_2 m)}(F) \qquad (10)$$

the function $\varepsilon^{(0,n-1,0)}(F)$ may be considered as an analytic continuation of energy of the state $|n-1,0,0\rangle$ to negative values of F.

Fig.1 shows the limiting curves, $n = \infty$, which were

obtained by independent calculation with the WKB method, see Sec.6. These curves qualitatively agree with the results of the calculations for finite but large n [2]. The dashed curve in Fig.1 determines the values of classical ionization threshold, see below Sec.7.

Analogous computations were carried out for $|n_1,n_1,0\rangle$ states with $n_1 = (n-1)/2$ and $n = 1,3,5,\ldots$. The linear Stark effect is absent for these states as well as for the states $|0,0,m\rangle$ and the energy is expanded in integer powers of F^2. The results of the computation are shown in Fig.2a and 2b. It is seen from the figures that with n increasing the values of $\mathcal{E}'_n$ converge very fastly to the limiting curve $\mathcal{E}_\infty$ determined by the WKB method. For instance the curves with $n_1 = 10$ and $n_1 = 15$ in Fig.2a are indistinguishible within the accuracy of the figure from one another and from the limiting curve $n_1 = \infty$. This is a much more fast convergence than that of previously considered $|0,0,n-1\rangle$ states, cf. Fig.2 with Fig.1 of ref. [17].

To explain this fact let us turn to eq.(4). If we choose a set of states $|n_1,n_2,m\rangle$ with fixed values of $\varkappa$ and μ, then PS coefficients $\mathcal{E}_k$ and the energy $\mathcal{E}(F)$ may be expanded at $n \to \infty$ in powers of $1/n^2$, i.e. the first correction to $\mathcal{E}_\infty(F)$ is of order $1/n^2$. This is just the case for the $|n_1,n_1,0\rangle$ where $\varkappa = \mu = 0$. At the same time, for other states at hand

$$\varkappa = 0\,, \quad \mu = 1 - n^{-1} \qquad \text{for} \quad |0,0,n-1\rangle$$

$$\varkappa = 1 - n^{-1}\,, \quad \mu = 0 \qquad \text{for} \quad |n-1,0,0\rangle$$

$$\varkappa = -1 + n^{-1}, \quad \mu = 0 \qquad \text{for} \quad |0, n-1, 0\rangle$$

Thus, the terms of order of n^{-1} emerge here from the parameters $\varkappa$ and μ themselves.

PS coefficients for excited states with n=2 and 3 have been obtained earlier [9,10]. Making use of these coefficients we summed the corresponding PS by means of HPA. The results are shown in Fig.3 (see also Fig.4 in ref. [20]).

5. It is convenient to represent the width of atomic levels as follows

$$\Gamma^{(n_1 n_2 m)} = \tilde{\Gamma}^{(n_1 n_2 m)}(F) \cdot \exp\left\{-n \delta_{n_1 n_2 m}(F)\right\} \qquad (11)$$

where the first factor $\tilde{\Gamma}^{(n_1 n_2 m)}$ corresponds to the quasi-classical equation [3]

$$\tilde{\Gamma}^{(n_1 n_2 m)} = A_{n_1 n_2 m} F^{-(n - n_1 + n_2)} \exp\left(-\frac{2n}{3F}\right) \qquad (12)$$

This equation is asymptotically exact in the limit $F \to 0$ and thus $\delta_{n_1 n_2 m}(0) = 0$,

$$\delta_{n_1 n_2 m}(F) = c_1 F + c_2 F^2 + \ldots, \quad F \to 0 \qquad (12')$$

The constants $A_{n_1 n_2 m}$ and $c_1, c_2, \ldots$ depend on quantum numbers, see Appendix A. Thus, for the ground state [2,10]: $A = 4$, $c_1 = 107/12$, $c_2 = 227/16$, and so on.

The values of Stark shifts computed by the described above methods are given in Figs.4,5. These figures refers mainly to the region $F > F_*$ where the atom ionization process is no more tunneling, see below Sec.7. Note that in this region of F the field strength dependence of level is close to linear. Dashed curves in Fig.4 corresponds to two first terms of 1/n expansion, $\mathcal{E}^{(0)} + \mathcal{E}^{(1)} n^{-1}$, and demonstrate that convergence of 1/n expansion is good enough even for small n (analogous situation takes place in the case of funnel potential [22]). Note that Fig.1 together with Fig.5 determine real and imaginary parts of energy for $|n-1,0,0\rangle$ and $|0,n-1,0\rangle$ states. The benefit of the reduced variables (1) is clear: owing to them the values of $\mathcal{E}_n$ for different levels have comparable magnitude and one may easily reveal regularities specific for different sets of states.

In the $F \lesssim F_*$ region factorization(11) is convenient. The quantities $\delta_{n_1 n_2 m}(F)$ can be easily obtained from computed widths of levels, see Fig.6a-c and Fig.3 of ref. [17] (for the $|0,0,n-1\rangle$ states).

At $F \to 0$ the only important factor in (11) is $\tilde{\Gamma}(F)$ strongly depending on the field and changing many orders of magnitude. But the applicability region of the asymptotics (12) is rather narrow for Rydberg states and is determined by the inequality $F < 0.1/n$ or $\mathcal{E} < 0.1\, n^{-5}$. In more intense fields the factor $e^{-n\delta}$ becomes very important and F-dependence of δ becomes essentially nonlinear. It should be noted that for all states [4] $\delta_{n_1 n_2 m}(F) > 0$, therefore ionization probability of a level by intense electric field is much smaller than the value which

follows from the estimate (12).

6 . The Rydberg limit. An equation for the energy eigenvalues for highly excited states follows from the quasiclassical Bohr-Sommerfeld quantization condition. In general case this condition envolves rather cumbersome elliptic integrals. If m = 0 and $n \to \infty$ these integrals may be evaluated analytically and quantization conditions take the form

$$\beta_1 F\left(\tfrac{1}{4},\tfrac{3}{4};2;-\frac{16\beta_1 F}{\varepsilon^2}\right) = (-\varepsilon)^{1/2}\nu_1 ,$$

$$\beta_2 F\left(\tfrac{1}{4},\tfrac{3}{4};2;\frac{16\beta_2 F}{\varepsilon^2}\right) = (-\varepsilon)^{1/2}\nu_2 , \qquad (13)$$

$$\beta_1+\beta_2 = 1 ,$$

where $\nu_i = (n_i+1/2)/n$, $\mu = m/n$ $(\mu+\nu_1+\nu_2=1)$ and $F \equiv {}_2F_1(\alpha,\beta;\gamma;z)$ is the hypergeometric function. Eqs.(13) may be solved numerically. Further simplification is possible if $n_1 = 0$ or $n_2 = 0$.

1) If $\nu_1 = 0$ (i.e., for $|0,n_2,0\rangle$ states, $n_2 \to \infty$) it may be shown that $\beta_1 \equiv 0$ at any F. Thus, eqs.(13) reduce to one equation

$$(-\varepsilon)^{1/2} = F\left(\tfrac{1}{4},\tfrac{3}{4};2;16F\varepsilon^{-2}\right) \qquad (14)$$

The energy ε remains real until $z = 16F/\varepsilon^2 < 1$. At $z=1$ the hypergeometric function has a branching point and the solution of the limiting , $n \to \infty$, equation (14) has a singularity

$$\varepsilon = \varepsilon_* \left\{ 1 + \tfrac{1}{2} f + \frac{2}{3} \frac{f}{\ln(-f)} + O\left(f \frac{\ln\ln f}{(\ln f)^2} \right) \right\} \tag{15}$$

where $F_* = \frac{2^{10}}{(3\pi)^4} = 0.1298$, $\varepsilon_* = \varepsilon(F_*) = -\frac{128}{(3\pi)^2} = -1.441$,

$$\varepsilon'' = c \frac{f}{\ln^2 f} \theta(f) + O\left(f \frac{\ln\ln f}{(\ln f)^3} \right) \tag{15'}$$

where $f = (F - F_*)/F_* \to 0$ and $c = -2\pi \varepsilon_*/3 = 3.018$. The corresponding curves ($n = \infty$) obtained by numerical solution of eq.(14) are shown in Figs.1,5.

2) Similarly, if $\nu_2 = 0$, then $\beta_2(F) \equiv 0$. For $|n_1, 0, 0\rangle$ states we get the equation

$$(-\varepsilon)^{1/2} = F\left(\tfrac{1}{4}, \tfrac{3}{4}; 2; -16 F \varepsilon^{-2}\right) \tag{16}$$

The energy ε becomes zero at $F = F_0$:

$$\varepsilon = \alpha_1 f + \alpha_2 f^2 + \alpha_3 f^3 + \dots , \tag{17}$$

where

$$F_0 = (2\gamma/9\pi)^2 = 0.383410 , \quad f = (F - F_0)/F_0 ,$$
$$\alpha_1 = \frac{\gamma^2}{27\pi} = 0.903 , \quad \alpha_2 = \frac{\gamma^2}{216\pi}\left(1 - \frac{\gamma^2}{48}\right) = -0.067 ,$$
$$\gamma = \left[\Gamma(1/4)/\Gamma(3/4)\right]^2 = 8.75376\dots \tag{17'}$$

Eq.(17) may be identically transformed to a more convenient form,

$$(\varepsilon^2+16F)^{1/4} = F\left(\tfrac{1}{2},\tfrac{5}{2};2;\tfrac{1}{2}\left[1+\frac{\varepsilon}{(\varepsilon^2+16F)^{1/2}}\right]\right) \qquad (18)$$

It is clear from (17) and (18) that $F=F_0$ is not a singular point for $\mathcal{E}(F)$. Moreover, $\mathcal{E}(F)$ remains real at all F from 0 to ∞ . Thus, for $|n_1,0,0\rangle$ states the level width vanishes [5] in the limit $n\to\infty$ which agrees with numerical calculations, see Fig.5.

3) For arbitrary state $|n_1,n_2,0\rangle$ with $\nu_2>0$ (and $n\to\infty$) the singularity of $\mathcal{E}(F)$ at $F=F_*$ is of the form indicated in (15).

7. The classical ionization threshold. As before $F < F_*$, the WKB equation (13) determines the real energy $\mathcal{E}(F)$; at $F > F_*$, $\mathcal{E}$ escape to complex plane. The quantity F_* is of a certain importance for the process of atom ionization by electric field, especially for Rydberh states. For states with $n_2=0$, $F = F_*$ is the value of the field corresponding to barrier vanishing in the effective potential $U_2(\eta)$.

The value of F_* depends on quantum numbers n_1,n_2,m (more precisely, in the limit $n\to\infty$, on the ratios ν_1 and ν_2) . The results of numerical calculations of F_* for some states are presented in Fig.7.

As was previously mentioned, in the region $0 < F < F_*$ tunneling is the origin of ionization of atomic states. At $F > F_*$ regime rather changes: exponential smallness of Γ disappears and expression (12) cannot represent F-dependence of

even in the zero approximation. It is interesting to note that beyond the classical ionization threshold, $F > F_*$, the F-dependence of $\Gamma^{(n_1 n_2 m)}$ is practically linear, see Figs. 4,5. The linear dependence of $\Gamma(F)$ is valid up to $F \sim 5$ and then the asymptotics $\Gamma^{(n_1 n_2 m)} \sim F^{2/3}$ for $F \to \infty$ comes into action.

It should also be noted that the calculated values of F_* considerably exceed the estimate which follows from the natural (at first sight) one-dimensional model[3]. Consider the tunneling of the electron along z axis, i.e. along the direction of electric field. The potential $V(z) = -z^{-1} - \mathcal{E} z$ has a maximum at $z_0 = \mathcal{E}^{-1/2}$ with $V(z_0) = -2\mathcal{E}^{1/2}$. Neglecting the Stark shift, we determine from condition $V(z_0) = -1/2n^2$ the moment of the barrier disappearance, $F_c = 1/16 = 0.0625$ which is 3-6 times less than the true value $F_* = n^4 \mathcal{E}_*$. Such a discrepancy indicates that F-dependence of $\mathcal{E}$, β_1 and β_2 is very important (and in the end, the three-dimensional electron motion during ionization).

8. Rydberg states. Investigation of highly excited (Rydberg) states attracted much attention in the last few years[23-28]. Recently there were experimentally observed some resonances in the photoionization cross section in electric field which correspond to $n \approx 15 \div 30$ and are narrow enough even at $E > 0$. Kolosov has pointed out[29] a relationship between these resonances and Stark quasistationary states and has obtained their positions and widths numerically. We have computed the complex energies of such energies by an independent method (summation of PS by quadratic HPA). The obtained results are partly described below.

Among all n^2 states $|n_1,n_2,m\rangle$ with fixed n the most stable are $|n-1,0,0\rangle$ and their neighbouring with $n_1 >> n_2$. It is seen already from the asymptotics of the level width at $F \to 0$, see eq.(12). That is why just these states can exist even at positive energy. The results of the calculation are given in Fig.8 for Stark shifts $\mathcal{E}_n'$ and in Fig.9 - for the level widths. Fig.8 shows also the limiting curve with $n=\infty$ evaluated through eq.(7). The F-dependence of $\mathcal{E}'$ is nearly linear at $0.3 < F < 0.8$. At $F \approx 0.4 \div 0.5$ the real part of the energy eigenvalues reverses its sign and a quasistationary level with positive energy appears.

It is seen from Figs.5,9 that at fixed n and F the least ionization probability is for $|n-1,0,0\rangle$ states followed by $|n-2,0,1\rangle$ and then by $|n-3,0,2\rangle$ and $|n-2,1,0\rangle$ and so on. It should be noted in addition that the values of $\mathcal{E}_n''$ and especially of $\mathcal{E}_n'$ for the last pair of states are very close. It is not difficult to explain this fact taking into account the structure of PS. Indeed, consider a set of states with $2n_2 + m = \text{const}$ and $n_2, m \sim 1 << n$. All of them have the same $\varkappa$ value,

$$\varkappa = 1 - \frac{2n_2+m+1}{n} \qquad (19)$$

Therefore, according to eq.(4) the coefficients $\mathcal{E}_k$ for these states (and, consequently, sums of PS (2) as well) differ only starting from the terms of order $1/n^2$. On the other hand, $\varkappa = 1 - \frac{m+1}{n}$ for the set of states $|n-m-1,0,m\rangle$ with $m = 0,1,2,\ldots << n$, and that is why $\mathcal{E}_k$ and the reduced energy

eigenvalues differ already in the terms $\sim 1/n$. The simplest examples of states anomalously close to each other in variables (1) are:

$$\begin{aligned} &|n-2,1,0\rangle \text{ and } |n-3,0,2\rangle, \quad \varkappa = 1-3/n \\ &|n-3,1,1\rangle \text{ and } |n-4,0,3\rangle, \quad \varkappa = 1-4/n \\ &|n-3,2,0\rangle, \quad |n-4,1,2\rangle \text{ and } |n-5,0,4\rangle, \quad \varkappa = 1-5/n \end{aligned} \tag{20}$$

(see Fig. 8). For the fields $\mathcal{E} = 6.5$ and 8.0 kV/cm our calculations are in full agreement with the Kolosov's computation [29] performed by different method. Thus, the above procedure of PS summation is confirmed once more.

More detailed results for the Rydberg states of a hydrogen atom, including a comparison with experiment are contained in our forthcoming paper.

10. Concluding remarks

1) Similar to other quantum mechanical problems [30-32], PS divergence is not an obstacle for evaluating the energy eigenvalues if one uses an appropriate summation method. In this case application of HPA appears effective. This method is applicable, in principle, to an arbitrary state for which a large enough number of PS coefficients is computed [6].

2) To achieve a high precision when summing PS by HPA $_N^{(P)}$ it was necessary to take $N = 10 \div 15$, i.e. to introduce into calculation about 80÷100 PT orders. At such high k values PT coefficients E_k approach the asymptotics (5) determined by the Dyson [21] singularity of $E^{(n_1 n_2 m)}(\mathcal{E})$ at $\mathcal{E} \to 0$. Thus, we take this singularity into account at PS summation which seems

to be necessary for successful summation of divergent PS. Therefore the number of higher PS orders computed exactly (or, at least, with high precision) should be of order of some tens. Nowadays, such calculations are quite real in quantum mechanics but inaccessible for quantum field theory.

3) Both methods in view, HPA and 1/n-expansion, supplement each other and allow one to describe the whole domain of the parameters n and F of physical interest.

Appendix A

According to refs.[18,19] constant A entering eq.(12) is

$$A_{n_1 n_2 m} = \frac{(4n)^{n-n_1+n_2}\exp[3(n_1-n_2)]}{n_2!(n_2+m)!\,n^3}\,, \qquad m \geq 0 \quad (A.1)$$

Assuming $n_2 >> 1$ and applying the Stirling formula we get

$$A_{n_1 n_2 m} \approx \text{const}\cdot a^n n^{-\alpha}, \quad a = 4e\frac{(e/2)^{2(\nu_1-\nu_2)}}{(1-\nu_1)^{1-\nu_2}\nu_2^{\nu_2}}\,, \ \alpha > 0 \quad (A.2)$$

where $\nu_i = (n_i+1/2)/n$, i=1 or 2. This leads, at $F \to 0$ and $n >> 1$, to

$$\Gamma^{(n_1 n_2 m)} \approx \exp\left\{-n\left[\frac{2}{3F} + (1-x)\ln F - k_{\nu_1\nu_2}\right]\right\}$$

$$k_{\nu_1\nu_2} = \ln a = 2(1-\ln 2)x - (1-\nu_1)\ln(1-\nu_1) - \nu_2\ln\nu_2 + 1 + 2\ln 2, \quad (A.3)$$

$$x = \nu_1 - \nu_2 .$$

We quote the values of $k_{\nu_1\nu_2}$ and c_1 (see eq.(12')) for some states. For $|0,0,n-1\rangle$ states we have $x = 0$, $A = 2^{2n} n^{n-2}/n!$,

$$k = 1 + 2\ln 2 = 2.386\,, \quad c_1 = \frac{1}{12n^2}(33n^2+54n+20) \quad (A.4)$$

for $|n-1,0,0\rangle$ states : $x = 1 - n^{-1} \approx 1$, $A = 4\,e^{3(n-1)} n^{-2}$,

$$k = 3\,, \qquad c_1 = \frac{1}{12n^2}(48n^2+9n+50) \quad (A.5)$$

for $|0,n-1,0\rangle$: states: $x = -1$,

$$k = 4\ln 2 - 1 = 1.773\,, \quad c_1 = \frac{1}{12n^2}(42n^2+51n+14) \quad (A.6)$$

and for $|n_1,n_1,0\rangle$ states : $\varkappa = 0$, $A = 2^{2n} n^{n-3}/[(\frac{n-1}{2})!]^2$

$$k = 1+3\ln 2 = 3.079\,, \qquad c_1 = \frac{1}{12n^2}(51n^2+18n+38) \qquad (A.7)$$

(when computing c_1 we used the results by Damburg and Kolosov [12]). Finally, for $|n_1,n_2,0\rangle$ states

$$k = 3+(1-\varkappa)[\beta-\ln(1-\varkappa)]\,, \quad \beta = 3\ln 2-2 = 0.079 \qquad (A.8)$$

which coincides at $\varkappa = \pm 1,0$ with (A.5)-(A.7). It is easy to show that $k_{\nu_1\nu_2}$ achieves its minimum at $\nu_1 = 0$, $\nu_2 = 1$ and its maximum at $\nu_2 = 1-\nu_1 = 4e^{-3} = 0.1991\ldots$ ($\varkappa = 0.702$, $k_{max} = 3 + 8e^{-3} = 3.398$). Thus, the constant $k_{\nu_1\nu_2}$ in eq.(A.3) changes from ~ 1.8 to 3.4.

At $F \to 0$

$$\Gamma^{(n_1n_2m)}(\mathcal{E})/\Gamma^{(n-1,0,0)}(\mathcal{E}) =$$

$$= \frac{1}{n_2!(n_2+m)!}\left(\frac{4F}{e^3n}\right)^{2n_2+m}\left[1-\frac{3}{4}(2n_2+m)F+O(F^2)\right] \qquad (A.9)$$

Hence, the level widths fastly increase with quantum numbers n_2 and m increasing (at fixed n; n_2, $m \ll n$ and $F \ll 0.2n$). As follows from Fig.9, this property is valid in strong fields as well.

Appendix B

As $n \to \infty$, the Bohr-Sommerfeld quantization conditions are

$$\int_{\xi_0}^{\xi_1} d\xi \left(\frac{4\beta_1}{\xi} - \frac{M^2}{\xi^2} - F\xi + \varepsilon \right)^{1/2} = 2\pi \nu_1 ,$$

$$\int_{\eta_0}^{\eta_1} d\eta \left(\frac{4\beta_2}{\eta} - \frac{M^2}{\eta^2} + F\eta + \varepsilon \right)^{1/2} = 2\pi \nu_2 , \qquad (B.1)$$

$$\beta_1 + \beta_2 = 1$$

where ξ_i , η_i are turning points (after scaling $\vec{r} \to n^2 \vec{r}$ and so on). The integrals entering these relations are rather cumbersome elliptic integrals. The situation is simplified if m=0. We denote

$$I(\varepsilon, \lambda) = \int_0^{x_1} dx \left(\varepsilon - x + \frac{\lambda}{4x} \right)^{1/2} , \quad \lambda > 0 \qquad (B.2)$$

where $x_0 = 0$, $x_1 = \frac{1}{2}\left[\varepsilon + (\varepsilon^2 + \lambda)^{1/2} \right] > 0$. Putting first $\varepsilon < 0$, with the help of the integral representation of hypergeometric function we obtain

$$I(\varepsilon, \lambda) = 2^{-5/2} \pi (-\varepsilon)^{3/2} \left[z\left(\sqrt{1+z} - 1 \right) \right]^{1/2} \cdot F\left(-\tfrac{1}{2}, \tfrac{1}{2}; 2; \frac{1-\sqrt{1+z}}{1+\sqrt{1+z}} \right) \qquad (B.3)$$

where $z = \lambda / \varepsilon^2$. The Kummer quadratic transformation

$$F\left(-\tfrac{1}{2},\tfrac{1}{2};2;\tfrac{1-\sqrt{1+z}}{1+\sqrt{1+z}}\right)=\left(\frac{1+\sqrt{1+z}}{2}\right)^{1/2}F\left(\tfrac{1}{4},\tfrac{3}{4};2;-z\right)$$

leads to a considerable simplification:

$$I(\varepsilon,\lambda)=\frac{\pi}{8}\lambda(-\varepsilon)^{1/2}\,F\left(\tfrac{1}{4},\tfrac{3}{4};2;-\frac{\lambda}{\varepsilon^2}\right) \qquad (B.4)$$

Analogously,

$$\int_0^{x_1}dx\left(\varepsilon+x+\frac{\lambda}{4x}\right)^{1/2}=\frac{\pi\lambda}{8}(-\varepsilon)^{1/2}\,F\left(\tfrac{1}{4},\tfrac{3}{4};2;\frac{\lambda}{\varepsilon^2}\right) \qquad (B.5)$$

($x_1=-\frac{1}{2}(\varepsilon+\sqrt{\varepsilon^2-\lambda}>0$). The last two equations allow us to reduce the integrals (B.1) to the form (13).

Up to now we supposed $\varepsilon<0$ which corresponds to discrete spectrum. However, eqs.(B.4),(B.5) can be analytically continued to complex ε values as well. It is interesting that they keep physical meaning also at $\mathrm{Re}\,\varepsilon>0$ describing the energy and width of quasistationary states. The situation is analogous to the case of the Yukawa potential [22]. We use further the identities

$$\begin{aligned}F\left(\tfrac{\alpha}{2},\tfrac{\alpha+1}{2};\gamma;-tg^2\theta\right)&=\\&=(\cos\theta)^{\alpha}\,F\left(\tfrac{\alpha}{2},\tfrac{\beta}{2};\gamma;\sin^2\theta\right)=\\&=(\cos\theta)^{\alpha}\,F\left(\alpha,\beta;\gamma;\sin^2\tfrac{\theta}{2}\right),\end{aligned} \qquad (B.6)$$

$\gamma=(\alpha+\beta+1)/2$. Substituting here $\alpha = 1/2$, $\beta = 5/2$ and $tg\theta = -\lambda^{1/2}/\varepsilon$ we find

$$I(\varepsilon,\lambda) = \frac{\pi}{8}\lambda(\varepsilon^2+\lambda)^{-1/4} F(\tfrac{1}{2},\tfrac{5}{2};2;w),$$

$$w = \sin^2\frac{\theta}{2} = \tfrac{1}{2}\left[1+\frac{\varepsilon}{(\varepsilon^2+\lambda)^{1/2}}\right] \qquad (B.7)$$

$(0<w<1 \quad at \quad -1<\varepsilon<\infty)$.

When deriving this equation we supposed $\varepsilon<0$, but the result may be analytically continued to $\varepsilon>0$, contrary to eq.(B.4). Application of this identity immediately leads to eq.(18).

Note that the behaviour of $I(\varepsilon,\lambda)$ at $\lambda\to 0$ essentially depends on the sign of ε (this is due to the fact that $\lim_{\lambda\to 0} w = \theta(\varepsilon)$). For example,

$$I(-1,\lambda) = \frac{\pi}{8}(\lambda - \tfrac{3}{32}\lambda^2+\dots), \qquad (B.8)$$

$$I(1,\lambda) = \tfrac{3}{2}\left[1-\frac{1}{16}\lambda\ln\lambda+\mathcal{O}(\lambda)\right] \qquad (B.9)$$

and at $\varepsilon = 0$

$$I(0,\lambda) = C\lambda^{3/4}, \qquad C = \left(\frac{\pi}{4\sqrt{2}}\right)^{1/2}\Gamma(\tfrac{1}{4})/\Gamma(\tfrac{3}{4}) \qquad (B.10)$$

This follows from (B.7) if we take into account that

$$F(\alpha,\beta;\frac{\alpha+\beta+1}{2};\tfrac{1}{2}) = F(\tfrac{\alpha}{2},\tfrac{\beta}{2};\tfrac{\alpha+\beta+1}{2};1) = \frac{\pi^{1/2}\Gamma(\frac{\alpha+\beta+1}{2})}{\Gamma(\frac{\alpha+1}{2})\Gamma(\frac{\beta+1}{2})}$$

and can be as well obtained by a direct evaluation of integral (B.2) with $\mathcal{E} = 0$.

In conclusion we note that $(-\infty < \epsilon < \infty)$

$$I(\epsilon, \lambda) = |\epsilon|^{3/2} \cdot I\left(\operatorname{sgn}\epsilon, \frac{\lambda}{\epsilon^2}\right) =$$

$$= \begin{cases} \frac{\pi\lambda}{8}(-\epsilon)^{-1/2}, & \epsilon \to -\infty \\ \frac{2}{3}\epsilon^{3/2}, & \epsilon \to +\infty \end{cases}$$

Footnotes

1) We use atomic units, $\hbar = m = e = 1$. The unit of electric field strength is 1 a.u. $= m^2e^5/\hbar^4 = 5.142 \cdot 10^9$ V/cm. The principal quantum number is $n = n_1 + n_2 + m + 1$ and $m \geq 0$.
2) We computed such curves for $n = 30$ and $n = 50$. In the scale of Fig.1 they are almost undistinguishable from the limiting curves, $n = \infty$.
3) See refs. [2,18,19].
4) This statement refers to the region of moderately strong fields ($F \lesssim 3$).
5) The potential $U_1(\xi) = -\frac{\beta_1}{2\xi} + \frac{m^2}{8\xi^2} + \frac{1}{8}\mathcal{E}\xi$ is confining at all $\mathcal{E} > 0$. This property leads to the above mentioned nullification of $\mathcal{E}_n''$ for the states $|n_1,0,0\rangle$ in the limit $n_1 \to \infty$, see Fig.5. Namely, in this case $\nu_1 = \nu_2 = 0$ and $\beta_2(F) \equiv 0$. The first of eqs.(13) is the quasiclassical quantization condition in the potential $U_1(\xi) = -\frac{1}{2\xi} + \frac{1}{8}\mathcal{E}\xi$ (with only discrete spectrum) while the second equation in eq.(13) reduces to identity $0 \equiv 0$.
6) At really accessible values of $k \leq 100$ (k is PT order) there is a restriction on the applicability of HPA in the strong field region, $F \gtrsim 0.5$.
7) E.g., $\mathcal{S}_{00}(F) < 0$ for the $|0,0,m\rangle$ states at $F > 10.2$. The maximum of the function $\mathcal{S}_{\nu_1\nu_2}(F)$ is found at $F = F_m = 1/3,\ 2/3$ and ∞ for the states $|0,n_2,0\rangle$, $|0,0,m\rangle$ and $|n_1,0,0\rangle$ correspondingly (note that $F_m > F_*$).
8) That is, $\mathcal{S}(F_*)$ and $\mathcal{S}'(F_*)$ are finite and the second derivative turns to be infinite.

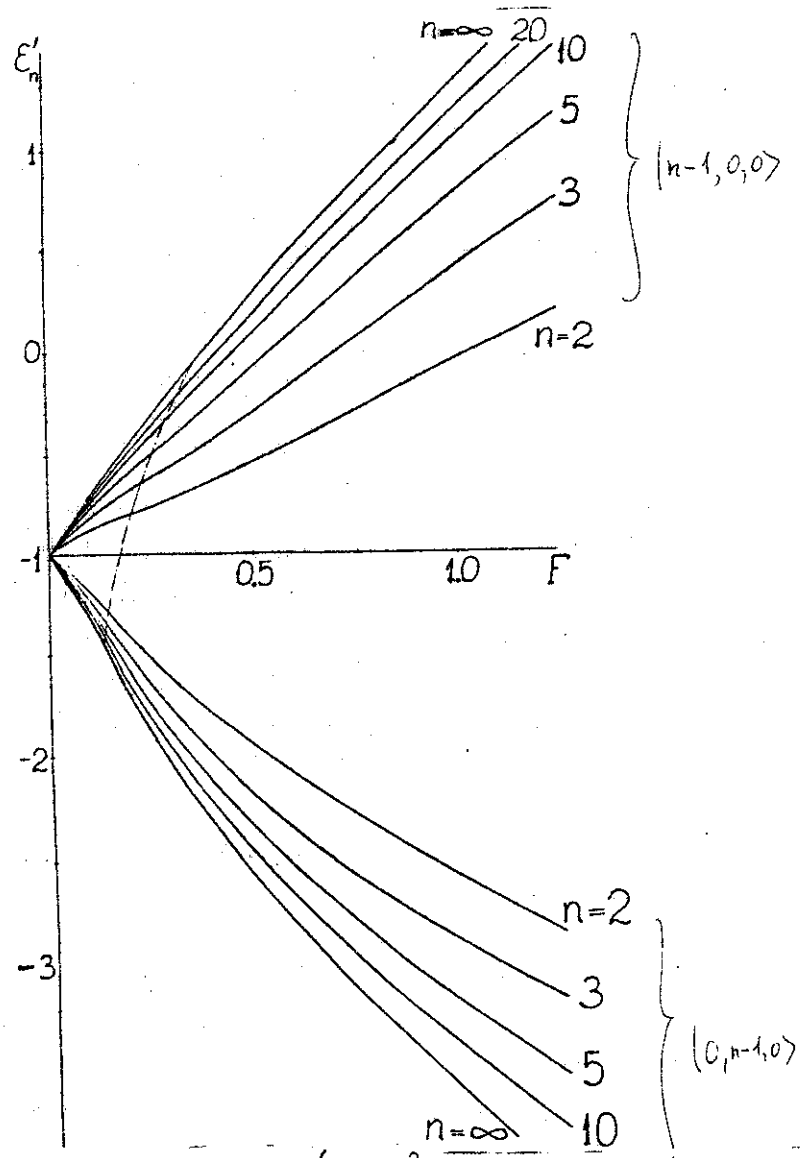

Fig.1. The values of $\mathcal{E}'_n = 2n^2 \mathrm{Re}\bar{E}$ for the states $|n-1,0,0\rangle$ and $|0,n-1,0\rangle$. The dashed line corresponds to the classical ionization threshold $F_*(\nu_1, \nu_2)$ for states with m=0, n >>1.

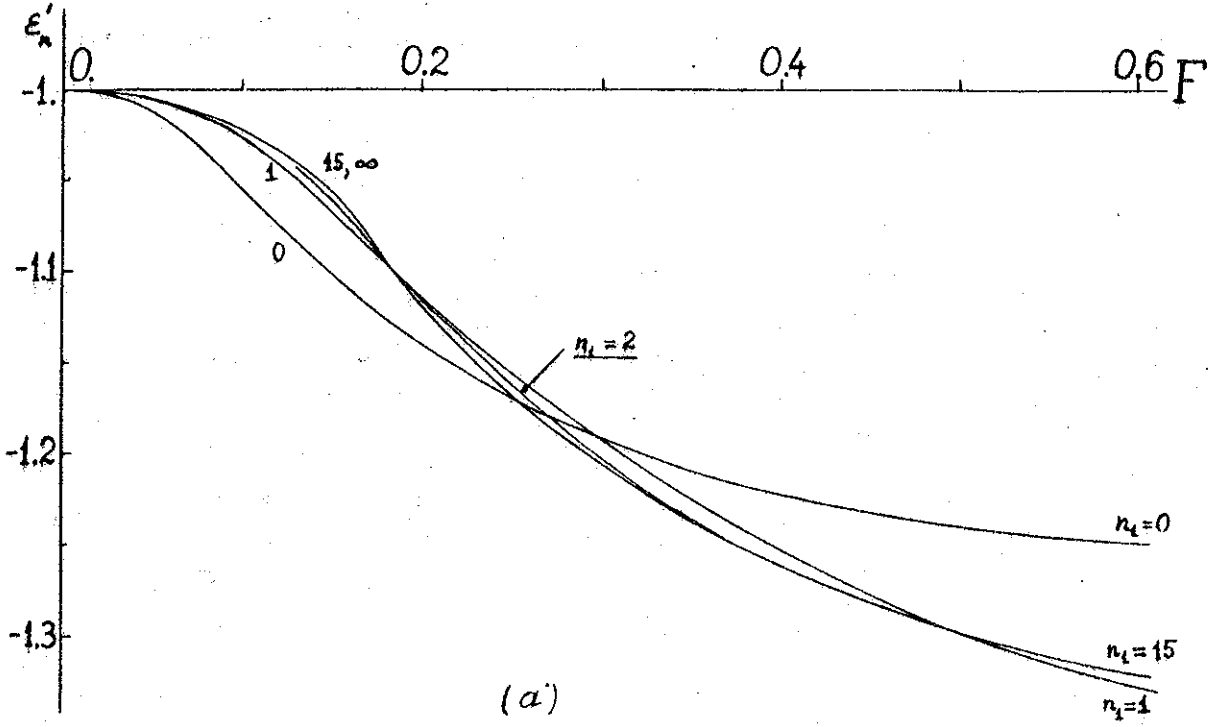

Fig. 2. The Stark shifts for states of the kind $|n_1, n_1, 0\rangle$ at $F < 0.6$

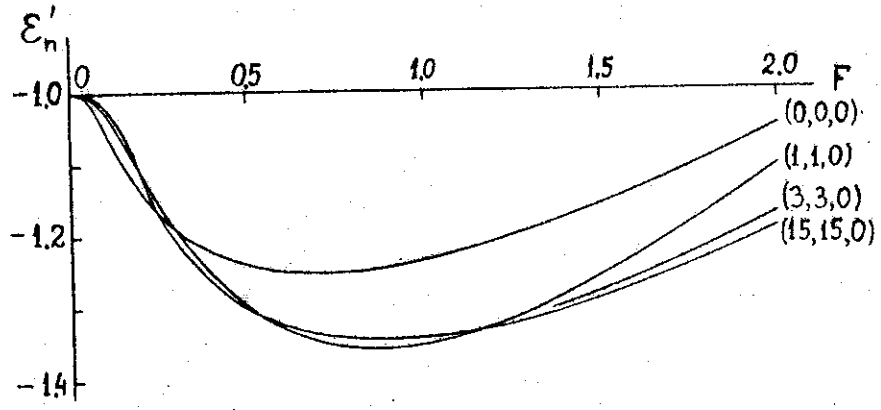

(b)

Fig.2b. The Stark shifts for states of the kind $|n_1,n_1,0\rangle$ at $0 < F < 2$. The values of n_1 are given at the curves.

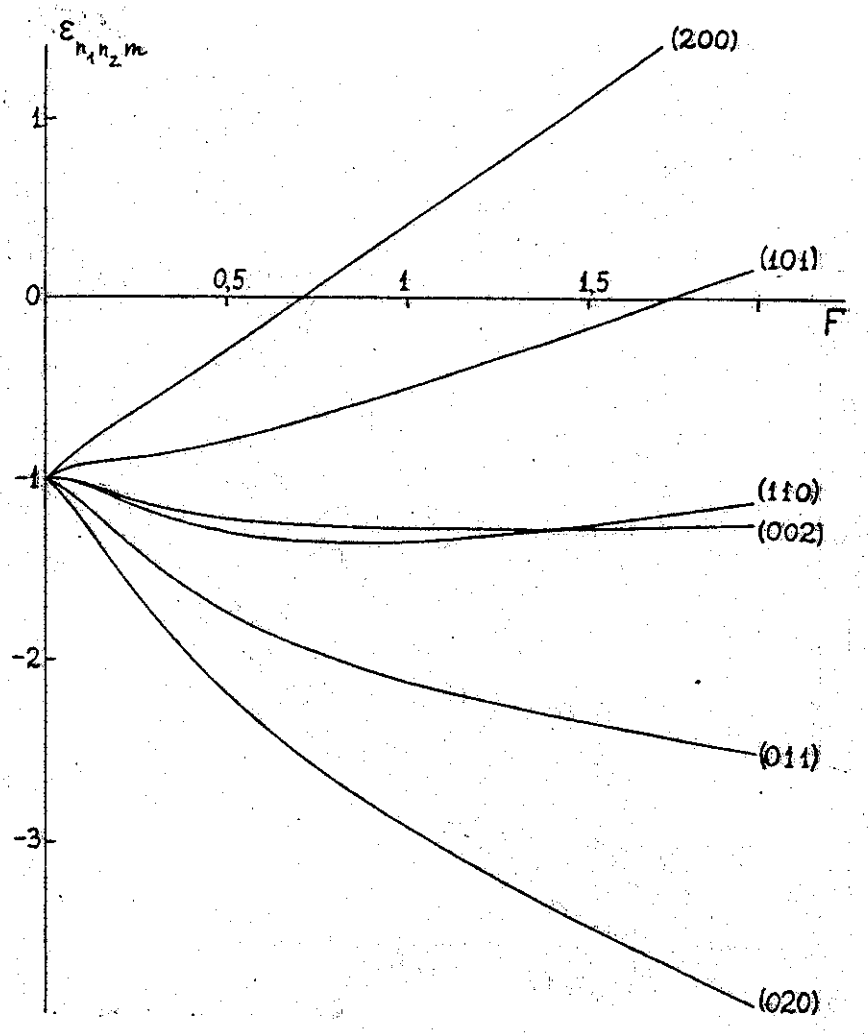

Fig.3. The Stark shifts of levels with n=3 ($F = 2\mathcal{E}/\mathcal{E}_a$, $\mathcal{E}_a$ = $5.142 \cdot 10^9$ V/cm). The curves are labeled by parabolic quantum numbers.

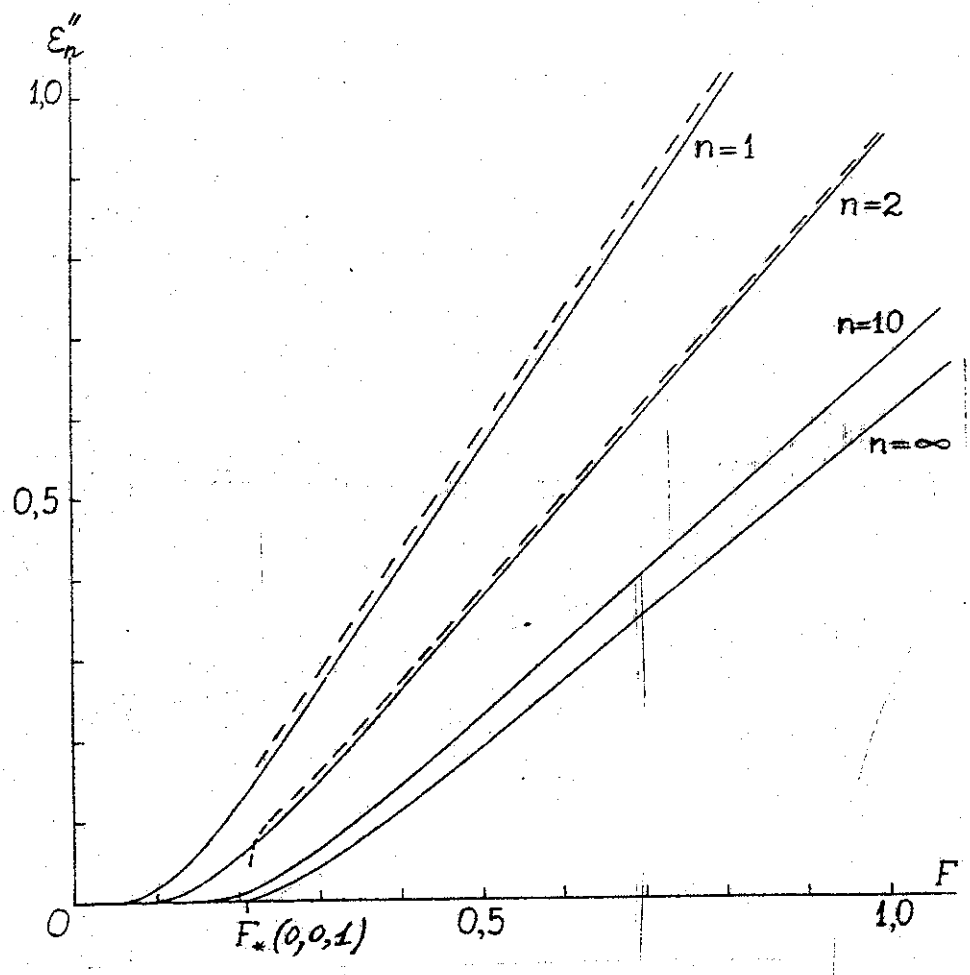

Fig.4. The electric field dependence of $\varepsilon_n'' = n^2 \Gamma^{(0,0,n-1)}$ for the states $|0,0,n-1\rangle$.

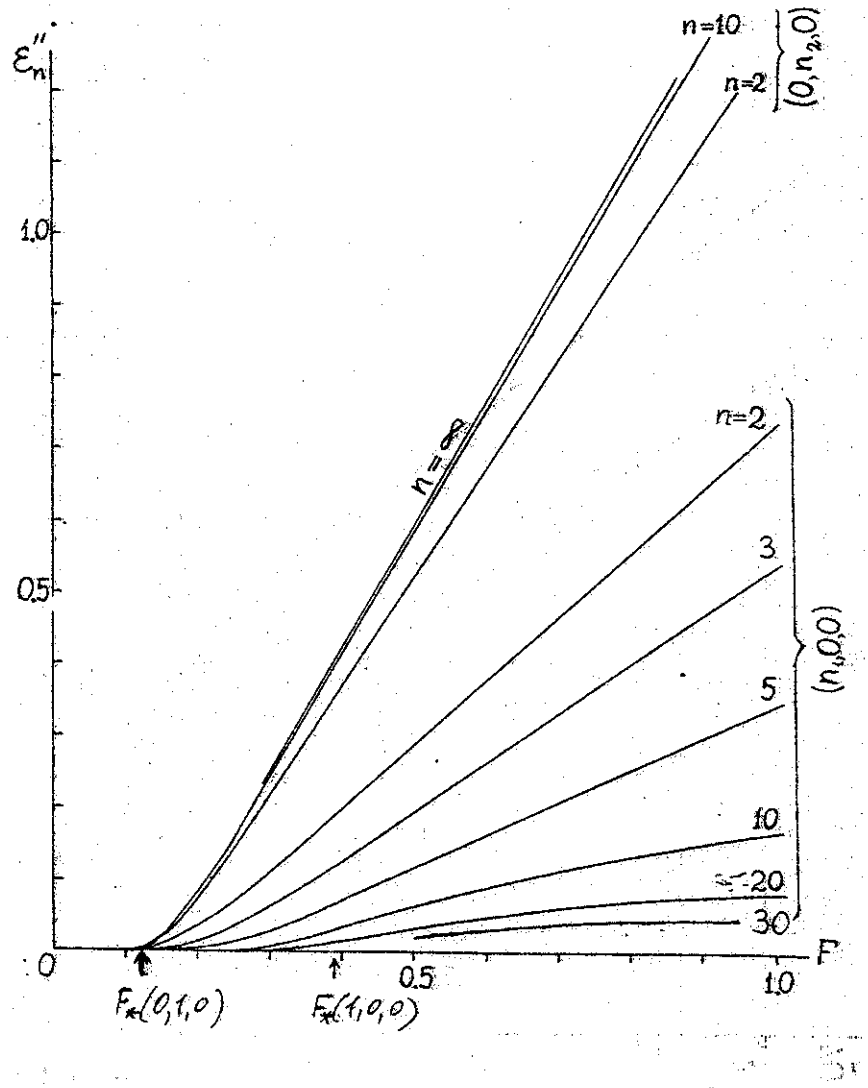

Fig.5a. The values of $\mathcal{E}_n'' = n^2 \Gamma^{n(n_1+n_2+n_3)}$ for the following states: $|n-1,0,0\rangle$ and $|0,n-1,0\rangle$

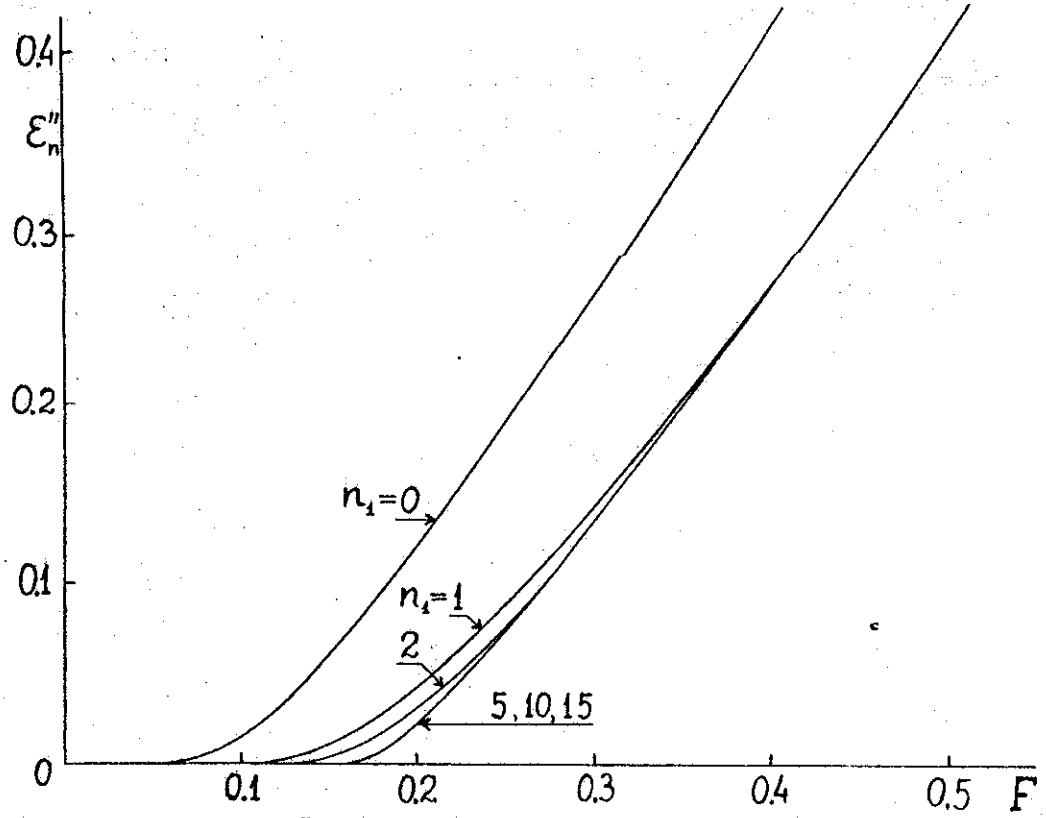

Fig.5b. The values of $\varepsilon''_n = n^2\Gamma(n_1,n_2m)$ for the following states: $|n_1,n_1,0\rangle$ with $n_1=(n-1)/2$, $n=1,3,5,\ldots$

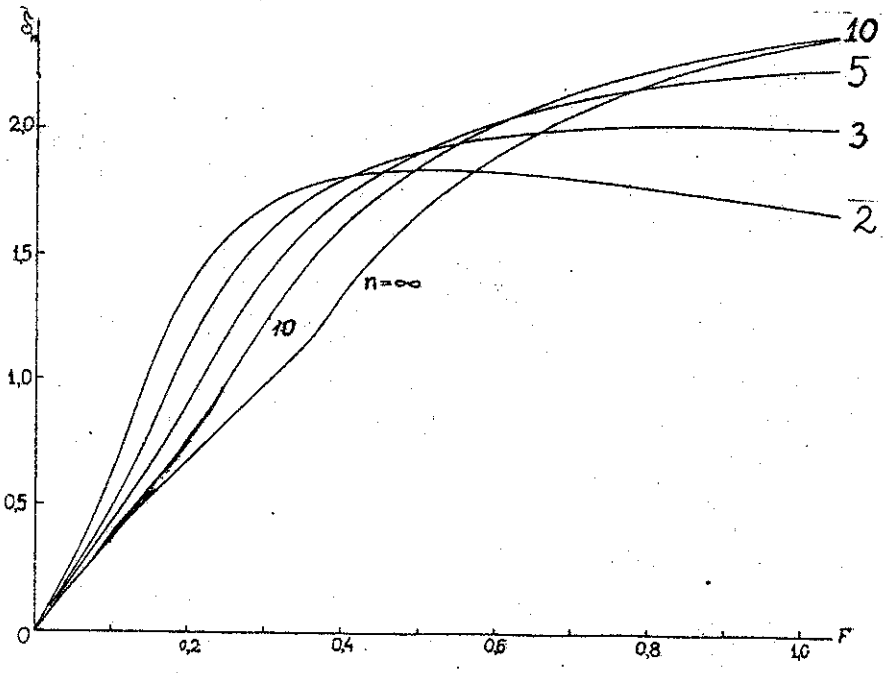

Fig.6a. Functions $\mathcal{S}_{n_1 n_2 m}(F)$, see eq.(11), for states $|n-1,0,0\rangle$;

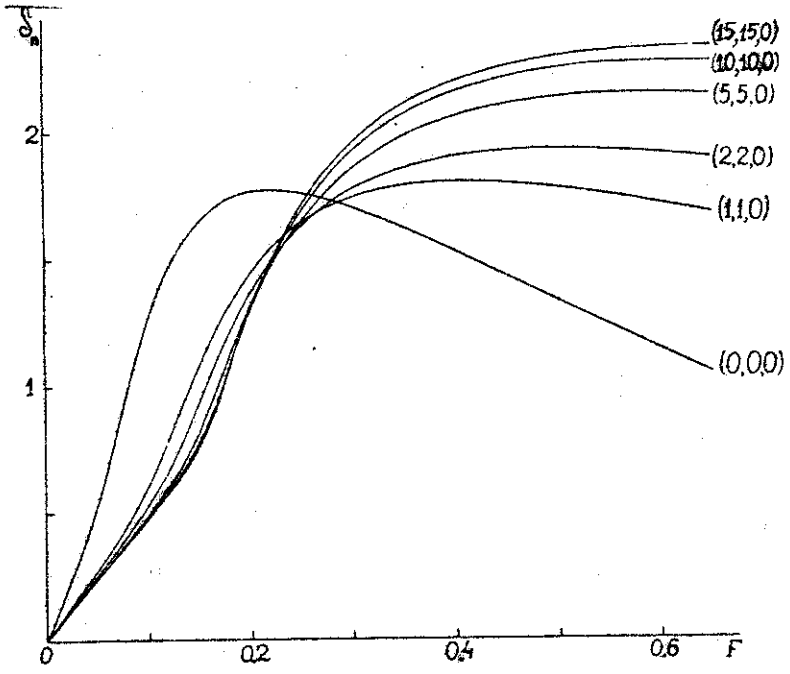

Fig.6b. Functions $\delta_{n_1 n_2 m}(F)$, see eq.(11), for states with $n_1 = n_2 = (n-1)/2$, $m=0$.

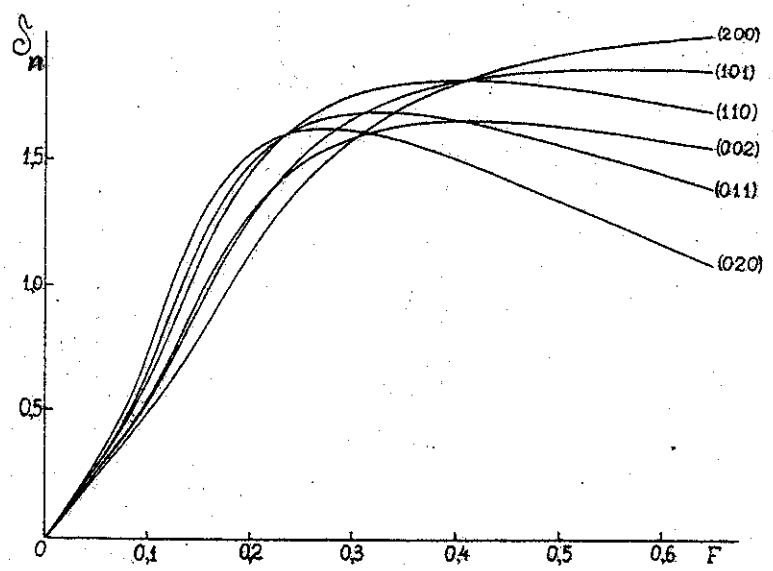

Fig.6c. Functions $\delta_{n_1 n_2 m}(F)$, see eq.(11), for all states with n=3.

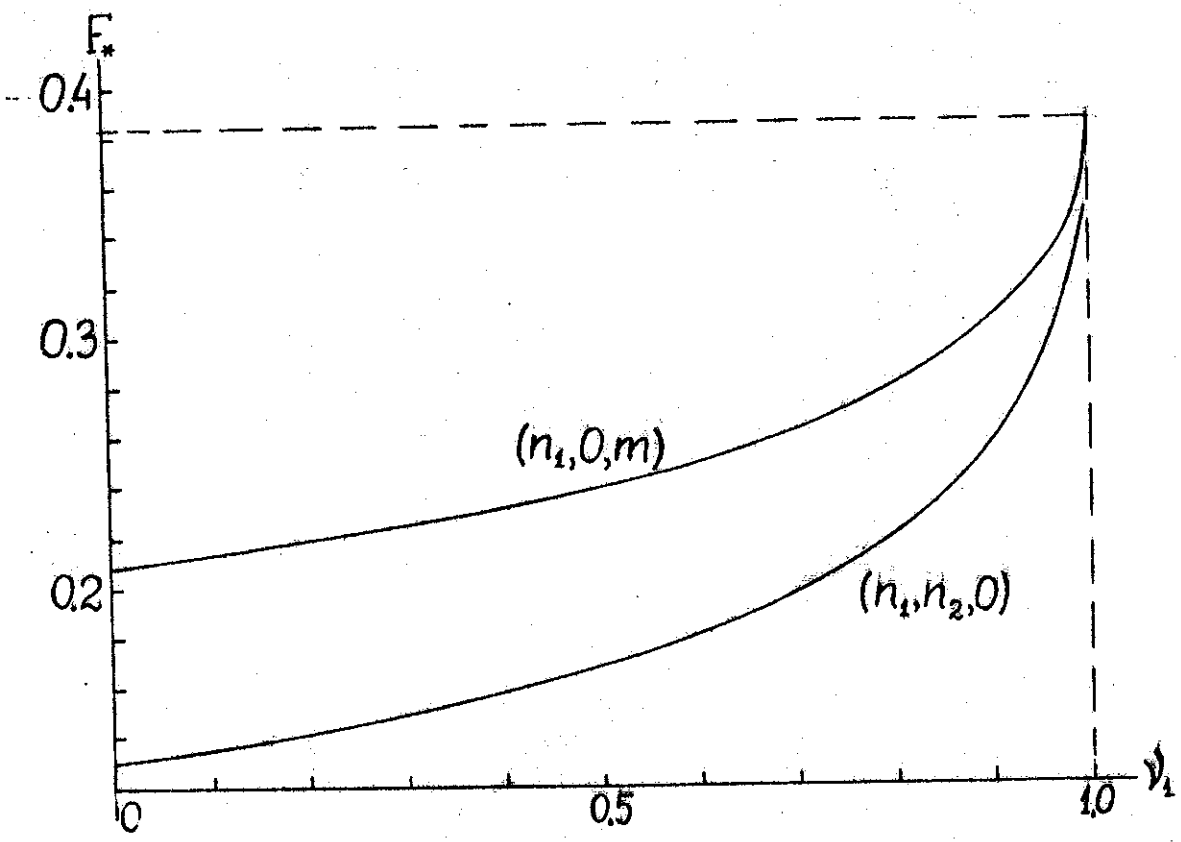

Fig.7. The classical ionization threshold F_* for some states of hydrogen atom; $\nu_1 = (n_1 + 1/2)/n$, $n \to \infty$.

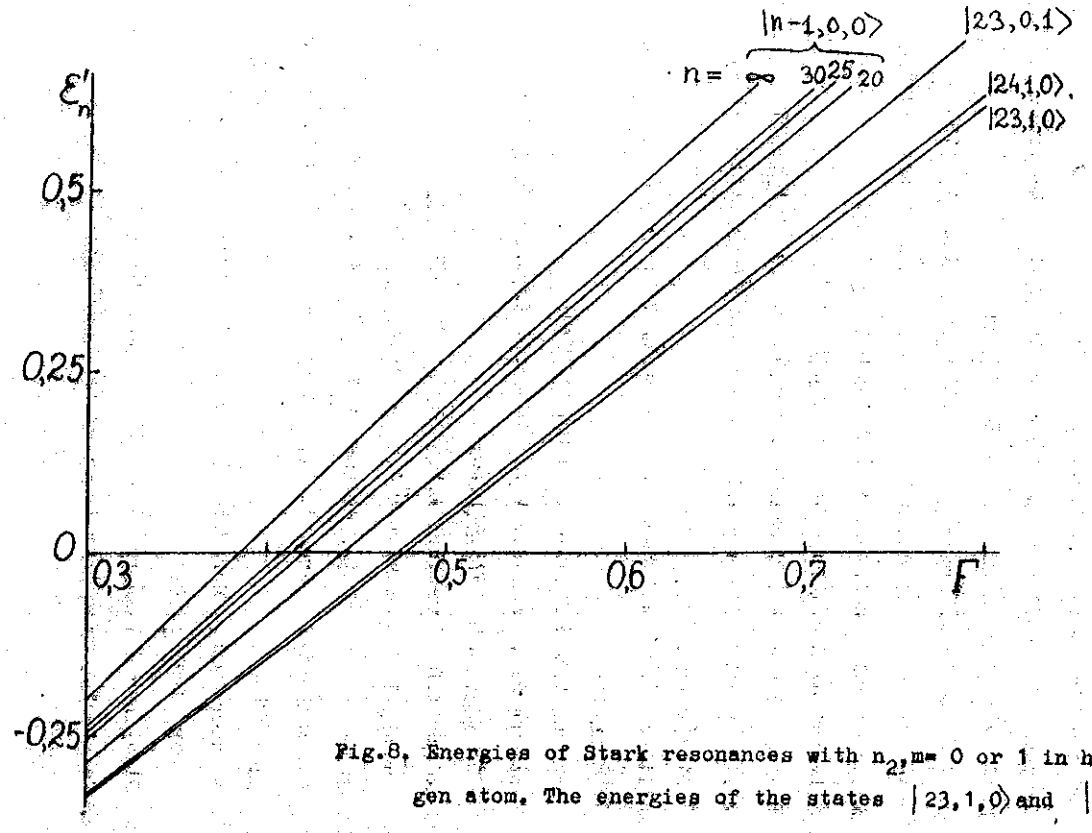

Fig.8. Energies of Stark resonances with n_2, m= 0 or 1 in hydrogen atom. The energies of the states $|23,1,0\rangle$ and $|22,0,2\rangle$ coincide up to the figure accuracy.

References

1. Bethe H.A., Salpeter E., Quantum Mechanics of Atoms with one and two Electrons, M.: Fizmatgiz, 1960.
2. Landau L.D., Lifshitz E.M., Quantum Mechanics. M: Nauka, 1974.
3. Mendelsohn L.B. // Phys.Rev., 1968, 176, 90.
4. Bekenstein J.D., Krieger J.B. // Phys.Rev., 1969, 188, 130.
5. Hehenberger M., McIntoch H.V., Brandas E. // Phys.Rev., 1975, A12, 1.
6. Alliluev S.P., Malkin I.A. // ZhETF, 1974, 66, 1283.
7. Silverstone H.J. // Phys.Rev., 1978, A18, 1853.
8. Hoe N., D'Etat B., Couland G. // Phys.Lett., 1981, 85A, 327.
9. Alliluev S.P., Eletsky V.L., Popov V.S. // Phys.Lett., 1979, 73A, 103; 1980, 78A, 43.
10. Alliluev S.P., Weinberg V.M., Eletsky V.L., Popov V.S. // ZhETF, 1982, 82, 77.
11. Privman V.L. // Phys.Rev., 1980, A22, 1833.
12. Damburg R.J., Kolosov V.V. // Journ.of Phys., 1976, B9, 3149; 1978, B11, 1921; 1979, B12, 2637.
13. Dolgov A.D., Turbiner A.V. // Phys.Lett., 1980, 77A, 15.
14. Benassi L., Grecchi V. // J.Phys., 1980, B13, 911.
15. Maquet A., Chu S.I., Reinhardt W.P. // Phys.Rev., 1983, A27, 2946.
16. Franceshini V., Grecchi V., Silverstone H.J. // Phys.Rev., 1985, A32, 1338.
17. Weinberg V.M., Mur V.D., Popov V.S., Sergeev A.V. // Pis'ma v ZhETF, 1986, 44, 9.
18. Slavyanov S.Yu. // Problemy Mat.Fiziki, 1970, 4, 125.
19. Yamabe T., Tachibana A. // Phys.Rev., 1977, 16, 877.

20. Popov V.S., Mur V.D., Weinberg V.M., Shcheblykin A.V. M., Preprint ITEP, 1986, No.125,

21. Dyson F.J. // Phys.Rev., 1952, 85, 631.

22. Popov V.S., Weinberg V.M., Mur V.D. // Pis'ma v ZhETF, 1985, 41, 439; Yad.Fiz., 1986, 44, 1103.

23. Rydberg states of atoms and molecules, ed.by R.F.Strebbings, F.B.Dunning, Cambridge Univ.Press, 1983.

24. Koch P.M. // Phys.Rev.Lett., 1978, 41, 99.

25. Koch P.M., Mariani D.R. // Phys.Rev.Lett., 1981, 46, 1275.

26. Glab W.L., Nayfeh M.H. // Phys.Rev., 1985, A31, 530.

27. Glab W.L., Ng K., Yao D., Nayfeh M.H. // Phys.Rev., 1985, A31, 3677.

28. Rottke H., Welge K.H. // Phys.Rev., 1986, A33, 301.

29. Kolosov V.V. // Pis'ma v ZhETF, 1986, 44, 457.

30. Eletsky V.L., Popov V.S., Weinberg V.M. // Phys.Lett., 1981, A84, 235; ZhETF, 1981, 81, 1567.

31. Popov V.S., Weinberg V.M. // Phys.Lett., 1982, A90, 107; 1985, A107, 371.

32. Weinberg V.M., Popov V.M. // Doklady Akademii Nauk SSSR, 1983, 272, 335.

В.С.Попов и др.
Эффект Штарка в сильном поле. II.
Работа поступила в ОНТИ 20.08.87

Подписано к печати 17.07.87 ТІ2І78 Формат 60x90 1/16
Офсетн.печ. Усл.-печ.л.2,25. Уч.-изд.л.1,6. Тираж 230 экз.
Заказ 177 Индекс 3624 Цена 24 коп.

Отпечатано в ИТЭФ, 117259, Москва, Б.Черемушкинская, 25

ИНДЕКС 3624

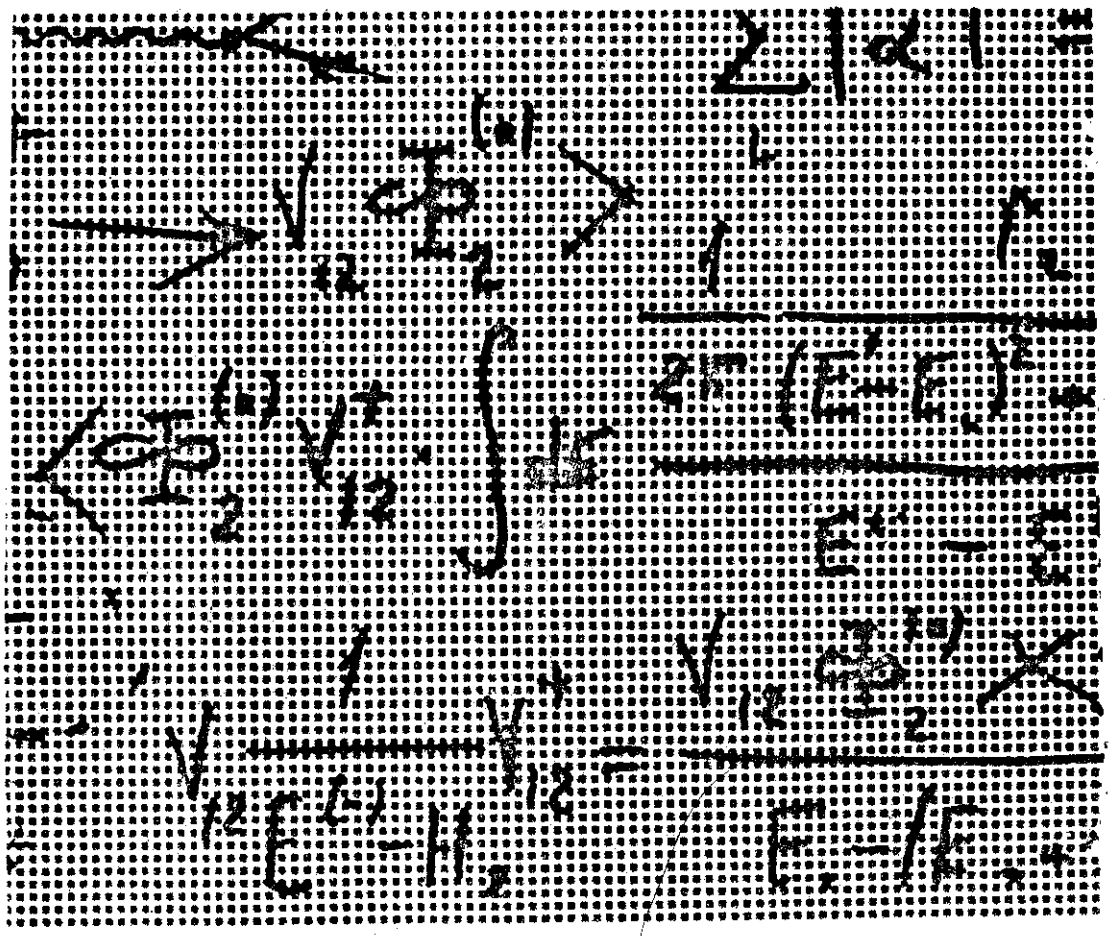

М.,ПРЕПРИНТ ИТЭФ, 1987, № 177, с.1-37